



Title	STRENGTH EVALUATION FOR A CORRODED DAMAGED STEEL GIRDER END CONSIDERING ITS COLLAPSE MECHANISM
Author(s)	USUKURA, M.; YAMAGUCHI, T.; SUZUKI, Y.; MITSUGI, Y.
Citation	Proceedings of the Thirteenth East Asia-Pacific Conference on Structural Engineering and Construction (EASEC-13), September 11-13, 2013, Sapporo, Japan, D-2-3., D-2-3
Issue Date	2013-09-12
Doc URL	http://hdl.handle.net/2115/54312
Type	proceedings
Note	The Thirteenth East Asia-Pacific Conference on Structural Engineering and Construction (EASEC-13), September 11-13, 2013, Sapporo, Japan.
File Information	easec13-D-2-3.pdf



[Instructions for use](#)

STRENGTH EVALUATION FOR A CORRODED DAMAGED STEEL GIRDER END CONSIDERING ITS COLLAPSE MECHANISM

M. USUKURA^{1*}, T. YAMAGUCHI^{2†}, Y. SUZUKI³, and Y. MITSUGI⁴

^{1,2}*Faculty of Engineering, Osaka City University, Japan*

³*Faculty of Engineering, Utsunomiya University, Japan*

⁴*Department of Civil Engineering, Ishikawa National College of Technology, Ishikawa, Japan*

ABSTRACT

In this study, FE analysis for the girder ends with corrosion has been carried out in order to understand the collapse process and to evaluate its ultimate strength. At first, the strength of the girder end with various corroded damages is evaluated based on the current design standards, “Specifications for Highway Bridges in Japan”. Secondly, these collapse mechanism are analyzed from the analytical results, such as shapes of the deformation mode, stress distribution, and load-deflection relationships and so on. Finally, we had summarized a flow diagram of a process of failure mode and the limit strength such as elastic, full-plastic and ultimate limit states taking into account for local buckling.

Keywords: Corrosion of girder ends, Collapse mechanism, Ultimate strength evaluation

1. INTRODUCTION

In recent years, it has been well known that some of steel bridges are deteriorated by corrosion at the girder ends as shown in Figure 1.



Figure 1: Examples of corroded girder ends

These are caused by stagnant water and sediment deposition due to water leakage, such as salt-laden from the expansion joint and airless environment. Various studies have been undertaken for how to evaluate decrease of the ultimate strength and how to repair corrosion damage of the girder end. At the present time, it has been almost cleared the collapse mechanism (Tamakoshi et al.2006;

* Corresponding author: Email: usukura@brdg.civil.eng.osaka-cu.ac.jp

† Presenter: Email: usukura@brdg.civil.eng.osaka-cu.ac.jp

Murakoshi et al.2010), but the evaluation method is not established considering the mechanism for load carrying capacity at the girder end with corrosion. In order to solve these technical issues, parametric analysis using FEM has been executed. It has been also discussed tendency of load carrying capacity decrease caused by corrosion damage at the bottom of stiffeners or the web plate adjacent the support.

2. FEM MODEL

2.1. MODEL

In this study, the FEM program ABAQUS has been used. As shown in Figure 2, the subject is a simple plate girder bridge end for national trunk roads which is shown in the standard design drawings of the 1994 version. As shown in Figure 3, forced vertical displacement is applied at the mid-span of the model where is between the intermediate and the end sway bracing in order to realize the actual loading condition of the girder end as much as possible. The model consists of a web panel, an upper and a bottom flange plate, vertical stiffeners, horizontal stiffeners, and a sole plate. The loading plate and the sole plate are modeled by solid elements, and other structural elements are modeled by shell elements. The corroded defect area is modeled by lack of FE elements. The material properties used are referred to the standard design specifications. The boundary conditions at the support are modeled as those for the line bearing. Since the residual stress due to welding might be released by loss of cross section due to corrosion, it is not considered. The initial deflection is not also considered because this research is a comparative study with parametric analysis. The used stress-strain relationship is assumed to be perfect elasto-plastic type, and the yielding function of von Mises is applied.

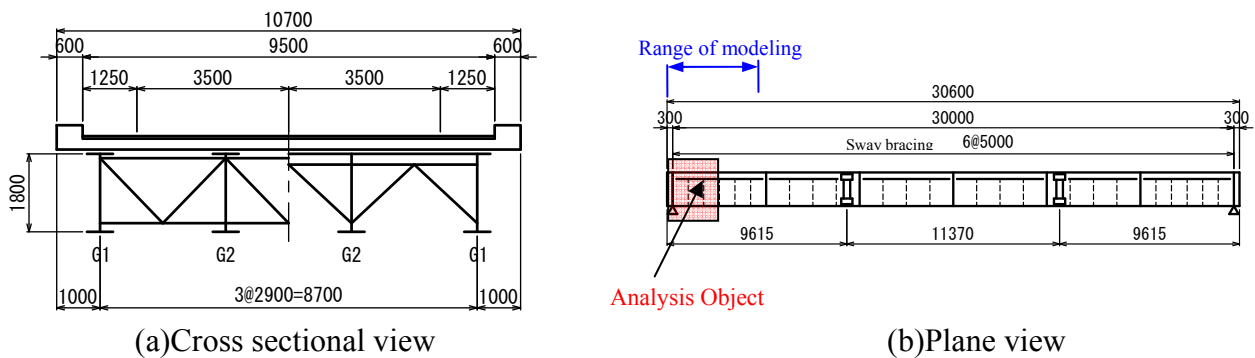


Figure 2: The objective girder end (unit :mm)

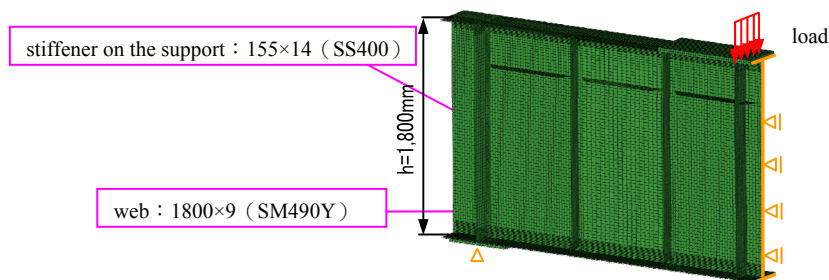


Figure 3: Overview of the model

Table 1: Design conditions of the bridge considered

Span	30(m)
Width	9.5(m)
Skew	90°
Live load	B Live load
Snow load	-
Slab thickness	250(mm)
Pavement thickness	80(mm)

Table 2: Geometrical configurations of the bridge

	Width (mm)	thickness (mm)	Steel grade
Stiffener on the Support	155	14	SS400
Web	-	9	SM490Y
Sole Plate(FIX)※	330	22	SS400

※Axial direction

2.2. PALAMETRIC ANALYSIS

In this study, an intact case and damaged cases in which the cross sectional loss areas are varied are dealt with. Summary of variation of cross sectional area at the support is shown in Figure 4. As shown in Figure 4, the deficit of the bottom of the web plate, one side or both sides of stiffeners are considered. The height of the deficit cross section is assumed constant, 10mm. In this study, an intact case is called as “Base model”. All analytical cases are tabulated in Table 3.

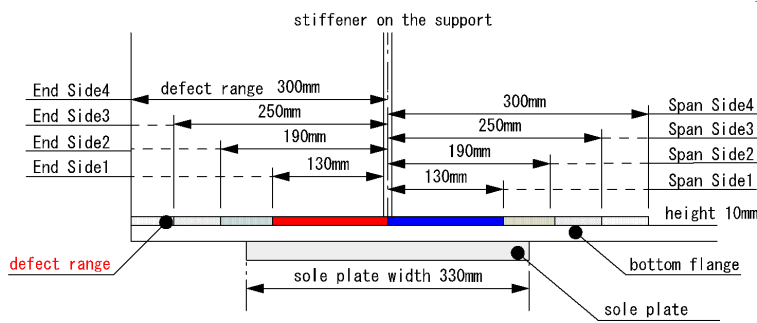


Figure 4: The used deficit parameters in the model

Table 3: Summary of analytical cases

case	Defect width
Base model	none
Web-deficient(Span Side1)	130mm
Web-deficient(Span Side2)	190mm
Web-deficient(Span Side3)	250mm
Web-deficient(Span Side4)	300mm
Web-deficient(End Side1)	130mm
Web-deficient(End Side2)	190mm
Web-deficient(End Side3)	250mm
Web-deficient(End Side4)	300mm
Stiffener-deficient (One side)	155mm
Stiffener-deficient (Both sides)	310mm

3. FEM RESULT AND DISCUSSION

3.1. ANALYSIS RESULTS

Figure 5 shows the load vs. relative displacement curves obtained.

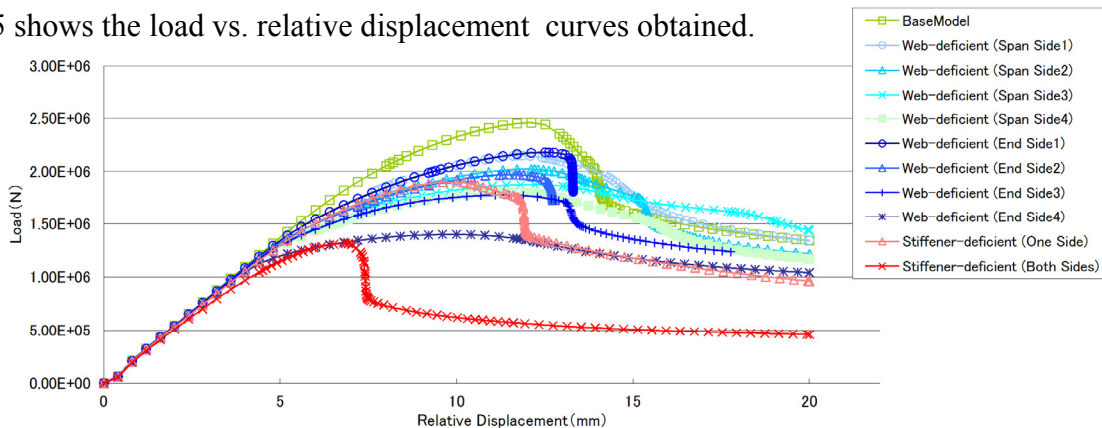


Figure 5: The load vs. relative displacement curves

Table 4 shows the maximum strength of each case obtained from the analysis and the reduction ratio to that of the Base model. For reference, the design strengths of the girder end with various corroded damages have been also evaluated by referring the current design standards, “Specifications for Highway Bridges in Japan”. These are calculated by the following equation.

$$P_d = \sigma_{caw} \cdot \nu \cdot A_{ew} + \sigma_{cas} \cdot \nu \cdot A_{es} \quad (1)$$

P_d : Design strength (N)

σ_{caw} : Allowable axial compressive stress for a web, 210 (N/mm²)

σ_{cas} : Allowable axial compressive stress for a stiffener, 140 (N/mm²)

ν : safety margin (=1.7)

A_{ew} : effective cross sectional area of a web (mm²), A_{es} : effective cross sectional area of a stiffener (mm²)

In the calculation, the safety margin is 1.7, the effective width of the web panel is 24t with exception of a cross sectional lack area.

It is found that the maximum strengths of all cases excepting Web-deficient case (End Side4) and Stiffener-deficient case (Both sides) exceed the design strength of the intact case (Base model). It means that the strength of the girder end with corrosion in which the height is less than 10mm is enough high with comparison of the original design strength.

The design strength considering lack of the cross section of Web-deficient case (End side4) is almost equal to the maximum strength. However, those of other cases are only 63% to 77% of each maximum strength. It is caused by the difference between the assumption of effective cross sectional area in the design strength calculation and the actual cross sectional area of a web panel.

Table 4: Analysis results (at the maximum strength)

Height deficit	Content	Deficit position	none	Web-deficient								Stiffener-deficient		
			Base Model	Span Side1	Span Side2	Span Side3	Span Side4	End Side1	End Side2	End Side3	End Side4	One side	Both sides	
			Defect width	0mm	130mm	190mm	250mm	300mm	130mm	190mm	250mm			300mm
0mm	P_{max} [maximum strength]	kN	2,460	—	—	—	—	—	—	—	—	—	—	—
	$P_{max}/P_{max}(\text{none})$		1.00	—	—	—	—	—	—	—	—	—	—	—
10mm	P_{max} [maximum strength]	kN	—	2,150	2,020	1,880	1,810	2,180	1,970	1,780	1,400	1,900	1,320	
	$P_{max}/P_{max}(\text{none})$		—	0.87	0.82	0.76	0.74	0.89	0.80	0.72	0.57	0.77	0.54	
Reference	P_d [design strength]	kN	1,710	1,365	1,365	1,365	1,365	1,365	1,365	1,365	1,365	1,200	690	
	P_d/P_{max}		0.70	0.63	0.68	0.73	0.75	0.63	0.69	0.77	0.97	0.63	0.52	

3.2. ANALYSIS OF THE COLLAPSE MODE

In this section, deformation diagrams, stress distributions and load vs. relative displacement curves are focused in order to analyze the collapse modes in detail considering shear buckling, local buckling, out-of-plane deformation and torsional deformation. In this study, local buckling is

defined as the buckling occurred at the bottom of the girder end. The effective width of a web as "column" is 12 times of a web thickness (= 216mm) from the support to both outer sides.

3.2.1. CLASSIFICATION OF COLLAPSE MODE

Figure 6 shows a flow diagram of the collapse mode. Some examples of the deformation and the stress distribution at the ultimate state are tabulated in Table 5. It is found from observation and the analysis of the analytical results that a collapse mode depends on the location and the amount of deficiency. Classification of the collapse modes are as follows;

Type 1 : Coupled buckling (symmetrical mode) :

Shear buckling at a web panel firstly, and then local buckling of all plate elements (both sides of a web panel and both sides of stiffeners), finally overall buckling of the column

Type 2 : Coupled buckling (web-asymmetrical mode) :

Shear buckling at a web panel firstly, and then local buckling of the plate elements (the one side web panel and both sides of stiffeners), finally overall buckling of the column

Type 3 : Local buckling at the bottom of the girder end:

Local buckling at the bottom of a web panel

Type 4 : Coupled buckling (stiffener-asymmetrical mode) :

Overall buckling of the column firstly, and then local buckling of the plate elements (both sides of a web panel and one of stiffeners)

Type 5 : Overall buckling at the column:

Plate buckling of a web panel

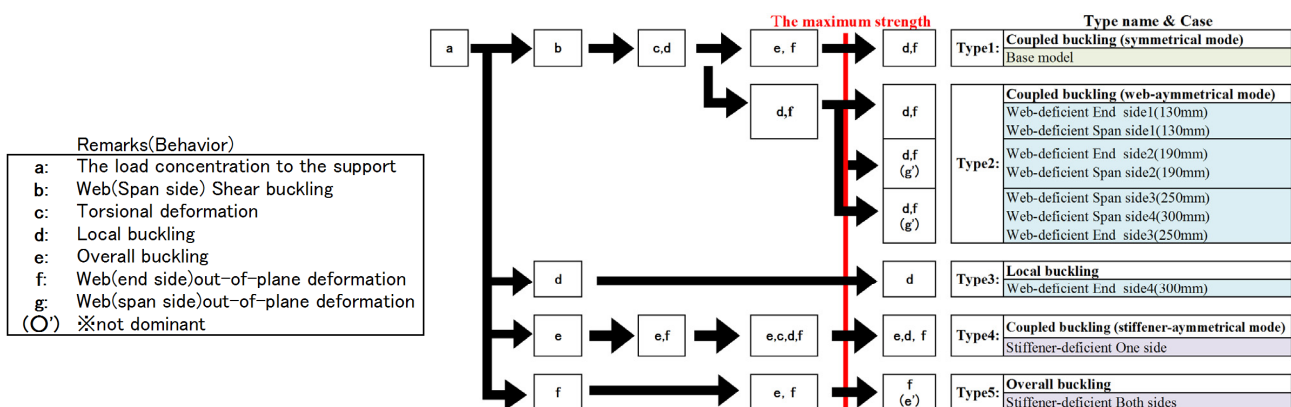


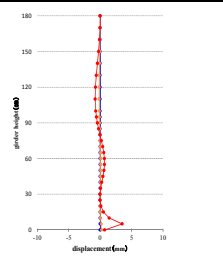
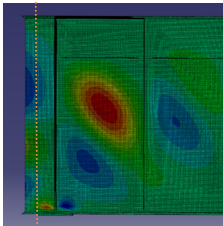
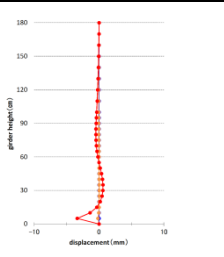
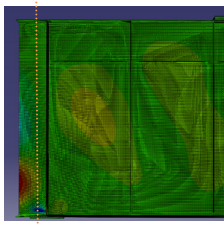
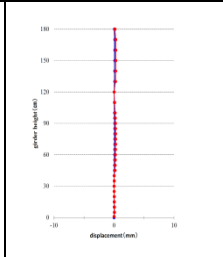
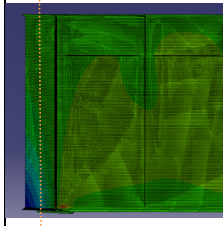
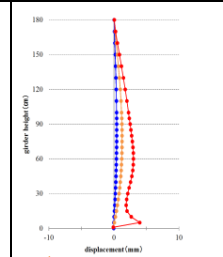
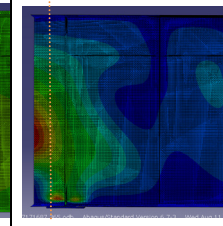
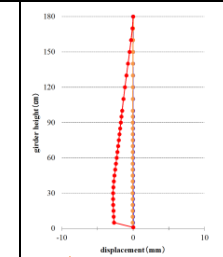
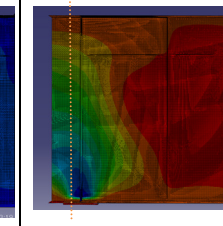
Figure 6: Classification of collapse mode

In case of Base model and Web-deficient cases with the exception of the Web-deficient case (End side4), shear buckling is firstly occurred at the span side web panel. Then, local buckling is occurred at the bottom of the end side web panel. By increase of the out-of-plane deformation of the "end side web panel", the column on the support, which consists of two stiffeners and the web panel, has been collapsed with the coupled buckling (Type 1 & 2). Such out-of-plane deformation of Base model is occurred at whole height of the girder. However, those of the Web-deficient cases are limited at the lower half height of the girder.

The larger the lack of the cross section of a web panel is, the smaller the deformation by shear buckling of a web panel at the span side web panel. As for the category of Type 2, out-of-plane deformation of the span side web panel is also observed at the maximum strength level due to the out-of-plane deformation of the end side web panel. In the case of Web-deficient case (End side4), local buckling is only observed at the bottom of the end side web panel, and shear buckling does not occur.

On the other hand, the collapse mode of Stiffener-deficient cases is different from the above cases. In this case, out-of-plane deformation at both sides of a web panel and an overall buckling of the column on the support have been occurred without a shear buckling of the web panel. In the case of Stiffener-deficient case (One side) (Type 4), the overall buckling of the column on the support is occurred with local buckling of the bottom of the web panel. As for Stiffener-deficient case (Both sides) (Type 5), it has collapsed by overall buckling of the web panel without local buckling deformation at the bottom of the web panel.

Table 5: Collapse mode list

	Type1	Type2	Type 3	Type 4	Type 5
	Coupled buckling (symmetrical mode)	Coupled buckling (web-asymmetrical mode)	Local buckling	Coupled buckling (stiffener-asymmetrical mode)	Overall buckling
deformation	 	 	 	 	 
Shear buckling	○	○	—	—	—
Local buckling	○	○	○	○	—
Overall buckling	○	○	—	○	○
case	Base model	Web-deficient • Span Side1,2, 3,4 • End Side1,2,3	Web-deficient • End Side4	Stiffener-deficient One side	Stiffener-deficient Both sides

※Deformation shapes at the cross-section and contours shown in this table are at the maximum strength. The cross section is apart from about 100mm to the support at an end side web panel.

3.2.2. EVALUATION OF VARIOUS LIMIT STRENGTHS

Table 6 shows various limit strengths (Initial yield strength, Full-plastic strength, Local buckling strength) which are extracted from the analytical results considering the mechanical behavior of the girder ends. The values in Table 6 are normalized by the maximum strength of each case. With exception of Type 3, each limit strength ratio to the maximum strength is almost same, though the lack location of the cross section is different among the cases. That is, initial yield strength is about 30~40%, full-plastic strength is about 70~80%, local buckling strength is about 90% respectively. The initial yield strength ratio of Type 3 is much higher than other types, but the Initial yield strength of Type 3 is almost same as other types.

Table 6: The dimensionless load at the limit strength

Limit strength	<i>The dimensionless load : each limit strength/maximum strength</i>									
	Type1	Type 2						Type 3	Type 4	Type 5
	Base model	Span side1	Span side2	Span side3	End side1	End side2	End side3	End side4	One side	Both sides
Initial yield strength	0.40	0.30	0.32	0.34	0.30	0.33	0.42	0.53	0.28	0.31
Full-plastic strength	0.70	0.75	0.77	0.81	0.71	0.76	0.81	0.91	0.75	0.73
Local buckling strength	0.89	0.87	0.90	0.91	0.92	0.89	0.89	0.97	0.98	—
Maximum strength	1.00	1.00	1.00	1.00	1.00	1.00	1.00	1.00	1.00	1.00

Note:

- i) Initial yield strength (perfectly elastic range) : the strength when a certain FE element on the web yields as shown in Figure 7
- ii) Full-plastic strength: the strength when yielding of the web panel reaches the effective area at the bottom of the web panel as shown in Figure 8.
- iii) Local buckling strength: the strength when local buckling occurs at the bottom of the girder ends near the support.

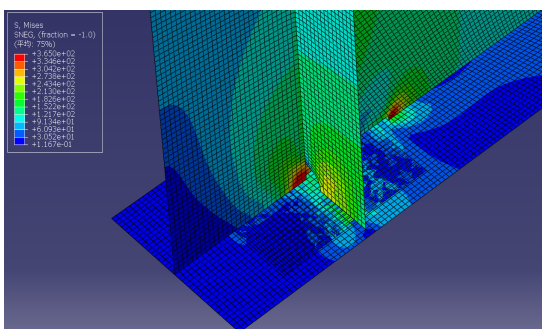


Figure 7: Examples of Initial yield strength Mises equivalent stress distribution

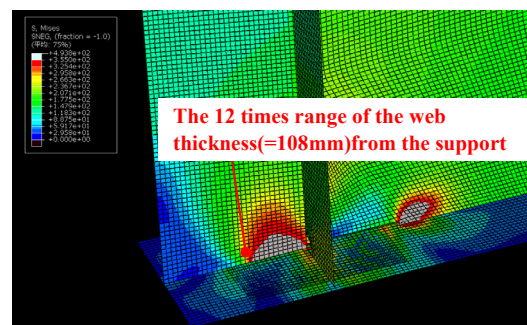


Figure 8: Examples of Full-plastic strength Mises equivalent stress distribution

Figure 9 shows each limit strength ratio to the design strength. The Initial yield strength of Base model (Type1) is about 60% of the design strength and it is almost 1.7 times of the design strength. This value is close to the value of the standard ultimate strength

curve considering a safety margin, 1.7. Although maximum strength of Type 2 and 4 are lower than that of Base model, their strength is higher than the design strength of base model. Strength increase rate to maximum strength from Full-plastic strength state for Type3 is relative small. In addition, elastic response range for Type 5 is smaller than that of other types and local buckling is not observed.

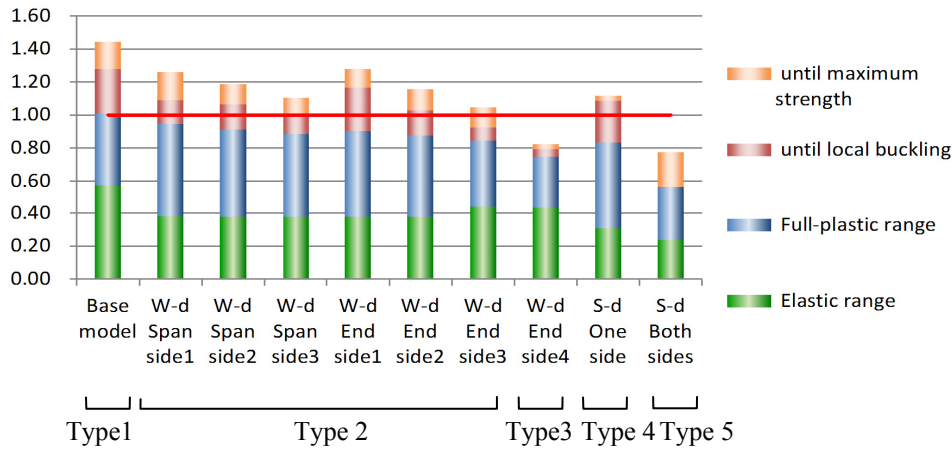


Figure 9: Summary of various limit strengths

4. CONCLUSIONS

In this study, are focused on the load carrying capacity and the collapse mechanism of the girder end at the support and FE analysis of it is performed for investigation. Obtained analytical results are as follows. :

- 1) Collapse mechanism of the girder end with corrosion damages is classified into five types based on the analytical results.
- 2) The various limit strengths of each case are compared with the corresponding to the design strengths. The strength reduction rate is estimated focusing on the collapse mechanism of each case. It was found that the out-of-plane deformation of the end side web panel has been caused by loss rigidity of the column on the support.

The future issue is to suggest the adequate formulation of strength based on the collapse mechanism.

REFERENCES

- Usukura M, Yamaguchi T, Toyota Y, Mitsugi Y , and Kondo A(2011). Influence of corrosion area of the girder ends of highway bridges to its load carrying capacity. *Journal of Structural Engineering* 57A, pp.724-734.
- Murakoshi J, Tanaka Y, Funaki K (2010) Studies on the anti-corrosion of the steel bridge girder ends , Documents Public Works Research Institute 4142, Japan
- Tamakoshi T, Nakasu K, Ishio M, Takeda T, Suizu N (2006) Resarch on local corrosion of Highway steel bridges, TECHICAL NOTE of National Institute for Land and Infrastructure No.294
- JAPAN ROAD ASSOCIATION(2012) ,SPECIFICATIONS FOR HIGHWAY BRIDGES PART II STEEL BRIDGES